Frontiers in Flow Cytometry™

A 24 hour Virtual Event by Thermo Fisher Scientific

Want to discover the latest advances in strategies & applications in flow cytometry?

Frontiers in Flow Cytometry is aimed at researchers across the globe looking for an opportunity to share current developments in flow cytometry.
Key topics include:

- Spectral and conventional flow cytometry
- Immunophenotyping
- Panel design and optimization
- Infectious diseases
- Advances in flow cytometry technology

This 24 hour virtual event will feature keynote presentations and industry colleagues, webinars, demos, live networking opportunities and more.

Join the conversation with your colleagues around the world. We are kicking off the event on May 17 at 8am SGT; 2am CEST; and 5pm PDT (May 16th).
#FrontiersInFlow

REGISTER NOW

 DOI: 10.1002/eji.201948368 Eur. J. Immunol. 2020. 50: 846–857

Basic

European Journal of Immunology

Tissue immunology and leukocyte trafficking

Research Article

IL-7 derived from lymph node fibroblastic reticular cells is dispensable for naive T cell homeostasis but crucial for central memory T cell survival

Laura Knop[*1], *Katrin Deiser*[*1], *Ute Bank*[1], *Amelie Witte*[1], *Juliane Mohr*[1], *Lars Philipsen*[1], *Hans J. Fehling*[2], *Andreas J. Müller*[1,3], *Ulrich Kalinke*[4] *and Thomas Schüler*[1]

[1] Institute of Molecular and Clinical Immunology, Medical Faculty, Otto-von-Guericke University, Magdeburg, Germany
[2] Institute of Immunology, University Clinics Ulm, Ulm, Germany
[3] Intravital Microscopy in Infection and Immunity, Helmholtz Centre for Infection Research, Braunschweig, Germany
[4] TWINCORE, Centre for Experimental and Clinical Infection Research, a joint venture between the Helmholtz Centre for Infection Research and the Medical School Hannover, Institute for Experimental Infection Research, Hannover, Germany

The survival of peripheral T cells is dependent on their access to peripheral LNs (pLNs) and stimulation by IL-7. In pLNs fibroblastic reticular cells (FRCs) and lymphatic endothelial cells (LECs) produce IL-7 suggesting their contribution to the IL-7-dependent survival of T cells. However, IL-7 production is detectable in multiple organs and is not restricted to pLNs. This raises the question whether pLN-derived IL-7 is required for the maintenance of peripheral T cell homeostasis. Here, we show that numbers of naive T cells (T_N) remain unaffected in pLNs and spleen of mice lacking *Il7* gene activity in pLN FRCs, LECs, or both. In contrast, frequencies of central memory T cells (T_{CM}) are reduced in FRC-specific IL-7 KO mice. Thus, steady state IL-7 production by pLN FRCs is critical for the maintenance of T_{CM}, but not T_N, indicating that both T cell subsets colonize different ecological niches in vivo.

Keywords: central memory T cells · fibroblastic reticular cells · IL-7 · naive T cells · T cell homeostasis

Additional supporting information may be found online in the Supporting Information section at the end of the article.

Introduction

IL-7 is indispensable for naive (T_N) and memory T cell (T_M) survival [1,2]. Correspondingly, IL-7-deficient (IL-$7^{-/-}$) mice suffer from severe lymphopenia [3] and adoptively transferred T_N fail to survive in such recipients [4]. Conversely, the administration of recombinant IL-7 supports T cell survival, e.g., via the upregulation of anti-apoptotic B-cell lymphoma-2 (Bcl-2) [1], myeloid cell leukemia-1 (Mcl-1) [5], and the promotion of metabolic functions [6–8].

Correspondence: Dr. Thomas Schüler
e-mail: thomas.schueler@med.ovgu.de

*These authors contributed equally to this work.

The maintenance of the T_N pool relies on the accessibility of secondary lymphoid organs (SLOs) where IL-7 is produced by lymphoid stromal cells (LSCs) [9]. In peripheral lymph nodes, for example, fibroblastic reticular cells (FRCs) and lymphatic endothelial cells (LECs) are the main sources of IL-7 [9]. Co-culture experiments demonstrated that FRC-derived IL-7 promotes T cell survival [9]. IL-7 binds to the ECM [10,11] suggesting that it might exert its function in close vicinity to the site of production. Due to the facts that T cell survival is impaired in vivo if either IL-7 action or peripheral LN (pLN) access is blocked [1,4,9,12,13], it has been proposed that circulating T_N receive IL-7-dependent survival signals in pLNs [14–17]. Since T_{CM} and T_N have similar migration patterns in vivo [18] and both rely on IL-7 [1,4], pLN FRCs are supposed to be critical for the IL-7-dependent persistence of both T cell subsets in vivo [15,17]. A potential contribution of LEC-derived IL-7 has been suggested as well [19].

However, various non-hematopoietic stromal cells express IL-7 [20–23] and its steady state levels vary strongly between different organs [24,25]. For example, intestine and skin produce high levels of IL-7 in the steady state while only low levels of *Il7* gene activity are detectable in the adult liver [24,25]. Since T_N and T_{CM} continuously recirculate between SLOs, blood, and lymph [26], they might utilize IL-7 derived from various organs. Hence, it remained unclear whether the maintenance of peripheral T cell homeostasis relies on the local action of IL-7 in pLNs and/or systemic effects of IL-7 produced by alternative sources.

In order to answer this question, we generated conditional IL-7 KO (IL-$7^{fl/fl}$) mice and inactivated *Il7* gene activity in a cell type-specific manner in pLNs. Here, we show that T_N numbers remained unaltered in pLNs and spleens of LEC- and FRC-specific IL-7 KO ($LEC^{\Delta IL\text{-}7}$ and $FRC^{\Delta IL\text{-}7}$) mice. In apparent contrast, T_{CM} abundance was significantly reduced in $FRC^{\Delta IL\text{-}7}$ mice, an effect that was most pronounced for $CD8^+$ T_{CM} in pLNs. In summary, we provide evidence that FRC-derived IL-7 is dispensable for the systemic survival of T_N cells. On the contrary, however, IL-7 produced by pLN FRCs is crucial for the maintenance of T_{CM} homeostasis indicating that T_N and T_{CM} occupy different ecological niches in vivo.

Results

Ubiquitous *Il7* gene inactivation impairs peripheral T cell homeostasis

In order to elucidate whether pLN-derived IL-7 is crucial for the maintenance of peripheral T cell homeostasis, we generated conditional IL-7 KO (IL-$7^{fl/fl}$) mice (Supporting Information Fig. 1A). IL-$7^{fl/fl}$ mice were crossed to conventional IL-7 KO (IL-$7^{-/-}$) mice [3] and mice ubiquitously expressing the loxP-specific recombinase Cre (PGK-Cre^+) [27] to obtain PGK-Cre^+IL-$7^{-/fl}$ mice. PGK-Cre-mediated inactivation of the $Il7^{fl}$ allele was very efficient as shown by the fact that *Il7* mRNA was undetectable in PGK-Cre^+IL-$7^{-/fl}$ mice (Supporting Information Fig. 1B).

Next, we compared the impact of conditional and conventional *Il7* gene inactivation on IL-7-dependent lymphocyte homeostasis. While mice harboring one intact $Il7^{wt}$ allele (PGK-Cre^-IL-$7^{-/wt}$, PGK-Cre^+IL-$7^{-/wt}$, and PGK-Cre^-IL-$7^{-/fl}$ mice) had comparable numbers of T and B cells in the spleen, ubiquitous *Il7* gene inactivation in PGK-Cre^+IL-$7^{-/fl}$ mice was associated with a strong decrease of T and B cell numbers similar to IL-$7^{-/-}$ mice (Fig. 1A). Importantly, the lack of IL-7 production in PGK-Cre^+IL-$7^{-/fl}$ and IL-$7^{-/-}$ mice was accompanied by the selective reduction of $CD44^{lo}CD62L^{hi}$ $CD4^+$ and $CD8^+$ T_N as well as the enrichment of $CD44^{hi}$ $CD4^+$ and $CD8^+$ memory T cells (T_M; Fig. 1B and C).

In summary, IL-7-dependent T cell homeostasis is similarly impaired in IL-$7^{-/-}$ and PGK-Cre^+IL-$7^{-/fl}$ mice thus confirming (i) the efficient Cre-mediated inactivation of the $Il7^{fl}$ allele and (ii) the crucial importance of IL-7 for T_N generation and maintenance. Hence, our IL-$7^{fl/fl}$ mouse is a suitable tool to study the impact of pLN-specific *Il7* gene inactivation on peripheral T cell homeostasis.

LEC-derived IL-7 is dispensable for peripheral T cell homeostasis

In pLNs, $CD45^-$ stromal cells comprise $gp38^+CD31^-$ FRCs, $gp38^+CD31^+$ LECs, $gp38^-CD31^+$ blood endothelial cells (BECs) and $gp38^-CD31^-$ double negative cells (DNs) [28] (Fig. 2A). Lyve-1-expressing LECs produce IL-7 in pLNs and throughout the body [29] and are supposed to be important regulators of IL-7-dependent peripheral T cell homeostasis [19]. In order to test this hypothesis, we generated $LEC^{\Delta IL\text{-}7}$ mice lacking *Il7* gene expression specifically in LECs. For this purpose, Lyve1-Cre-transgenic (Lyve1-Cre^+) mice [30] were crossed to IL-$7^{fl/fl}$ mice. Lyve1-Cre^+ mice harboring at least one intact *Il7* allele (LEC^{wt} mice) served as controls. $CD45^-$ stromal cells were purified from LNs of $LEC^{\Delta IL\text{-}7}$ and LEC^{wt} mice and relative *Il7* mRNA levels were quantified by RT-qPCR. In agreement with a previous report [9], LECs produced considerable amounts of *Il7* mRNA in control mice, even though tenfold less than FRCs (Fig. 2A). Of note, *Il7* mRNA levels were strongly reduced in LECs from $LEC^{\Delta IL\text{-}7}$ mice indicating successful *Il7* gene inactivation. On the contrary, *Il7* mRNA levels in FRCs, BECs, and DNs were comparable in $LEC^{\Delta IL\text{-}7}$ and LEC^{wt} mice.

In order to study whether LEC-derived IL-7 affects peripheral T cell homeostasis, $CD4^+$ and $CD8^+$ T cells were quantified in pLNs and spleens of $LEC^{\Delta IL\text{-}7}$ and LEC^{wt} mice. As shown in Fig. 2B, T cell numbers were indistinguishable between both mouse lines. Furthermore, relative frequencies and numbers of $CD44^{lo}CD62L^{hi}$ T_N, $CD44^{hi}CD62L^{lo}$ T_{EM}, and $CD44^{hi}CD62L^{hi}$ T_{CM} were comparable in pLNs and spleens (Fig. 2C–H), although $CD4^+$ T_{CM} frequencies were reduced in pLNs of $LEC^{\Delta IL\text{-}7}$ mice (Fig. 2C and D). In conclusion, *Il7* gene inactivation in LECs does not have major effects on quantitative and qualitative aspects of peripheral T cell homeostasis.

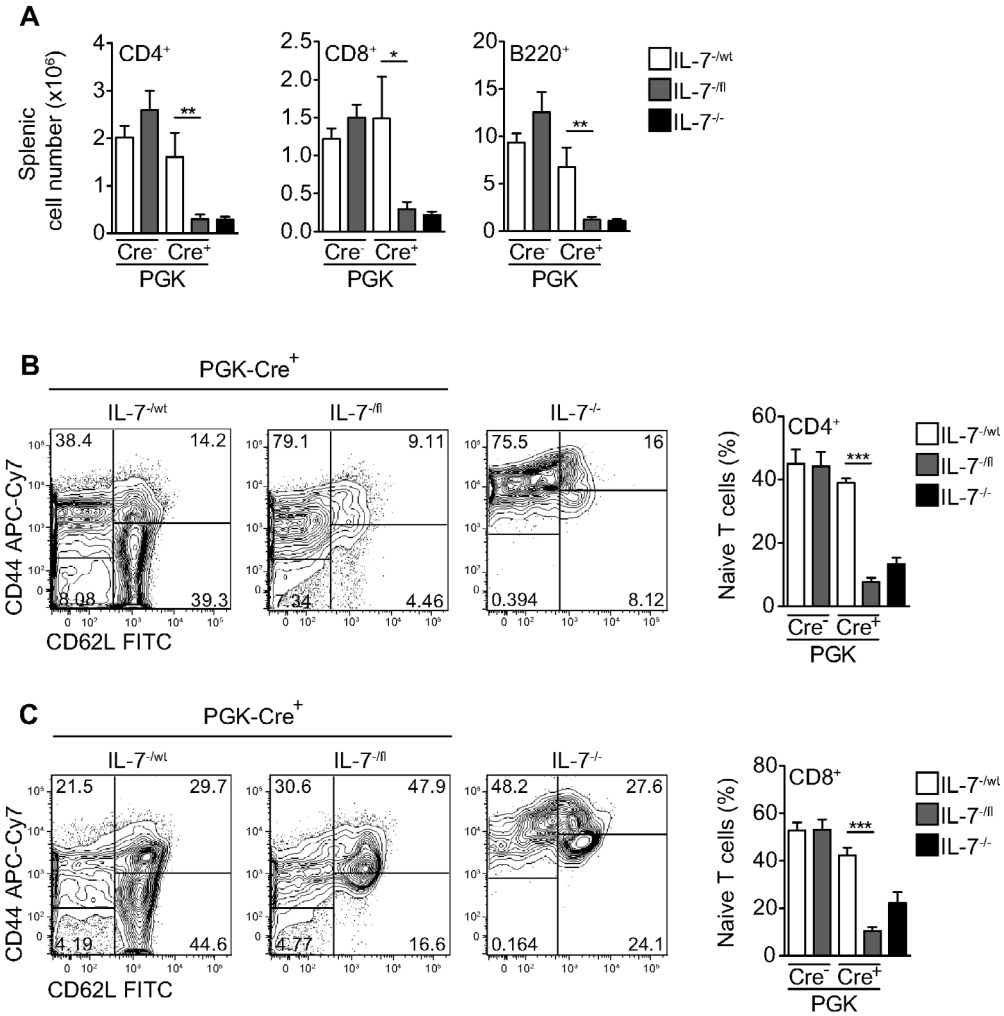

Figure 1. Ubiquitous *Il7* gene inactivation impairs T cell homeostasis. (A) Absolute cell numbers of $CD3^+CD4^+$ or $CD3^+CD8^+$ T cells and $B220^+$ B cells were determined in the spleen of the indicated mouse lines. (B and C) Shown are representative contour plots for the CD44/CD62L expression profiles of (B) $CD3^+CD4^+$ or (C) $CD3^+CD8^+$ T cells in spleen. Numbers in contour plots indicate percentages. Frequencies of naive (B) $CD3^+CD4^+CD44^{lo}CD62L^{hi}$ and (C) $CD3^+CD8^+CD44^{lo}CD62L^{hi}$ T cells are summarized in bar diagrams. (A–C) The data displayed in bar diagrams represent mean ± SEM of seven to nine mice per group analyzed in two independent experiments by flow cytometry. Statistical significances were tested using a non-parametric two-tailed Mann–Whitney *U*-test ($^*p \leq 0.05$; $^{**}p \leq 0.01$; $^{***}p \leq 0.001$).

FRC-derived IL-7 does not affect size and TCR diversity of the peripheral T cell pool

Prx1-Cre-transgenic (Prx1-Cre^+) mice express Cre in BM stromal cells [31], which are crucial for IL-7-dependent B cell development [32]. Whether this mouse model is suitable for targeting FRCs in pLNs was analyzed next. For this purpose, Prx1-Cre^+ mice were crossed to ROSA26 reporter mice expressing red fluorescent protein (RFP) upon Cre-mediated activation of the reporter construct [33]. Peripheral LNs of Prx1-$Cre^+$$ROSA26^{RFP}$ mice were analyzed by flow cytometry to determine the degree of cell type-specific recombination. Among $CD45^-$ stromal cells, around 80% of FRCs expressed RFP while LECs, BECs, and DNs showed only negligible levels of recombination (Fig. 3A and B). Of note, Cre activity was barely detectable in $CD45^+$ immune cells (Fig. 3A) as well as splenic LSCs (data not shown). Hence, Prx1-Cre^+ mice allow gene targeting in pLN FRCs.

In order to inactivate *Il7* gene activity in pLN FRCs, Prx1-Cre^+ mice were crossed to $IL\text{-}7^{fl/fl}$ mice. As compared to FRC^{wt} littermate controls, *Il7* mRNA levels were reduced by approximately 83% in pLNs of $FRC^{\Delta IL\text{-}7}$ mice (Fig. 3C) confirming that FRCs are the major source of IL-7 in pLNs. In contrast, *Il7* mRNA levels in the spleen of $FRC^{\Delta IL\text{-}7}$ mice remained unaltered (Fig. 3C), probably due to the different developmental origins of splenic and LN FRCs [34,35]. Importantly, FRC-specific *Il7* inactivation did not affect frequencies of LSC subsets (Fig. 3D), overall morphology, and chemokine secretion in pLNs (Supporting Information Fig. 2A–D).

When $CD4^+$ and $CD8^+$ T cells were quantified in pLNs and spleens of $FRC^{\Delta IL\text{-}7}$ and FRC^{wt} mice, no significant differences

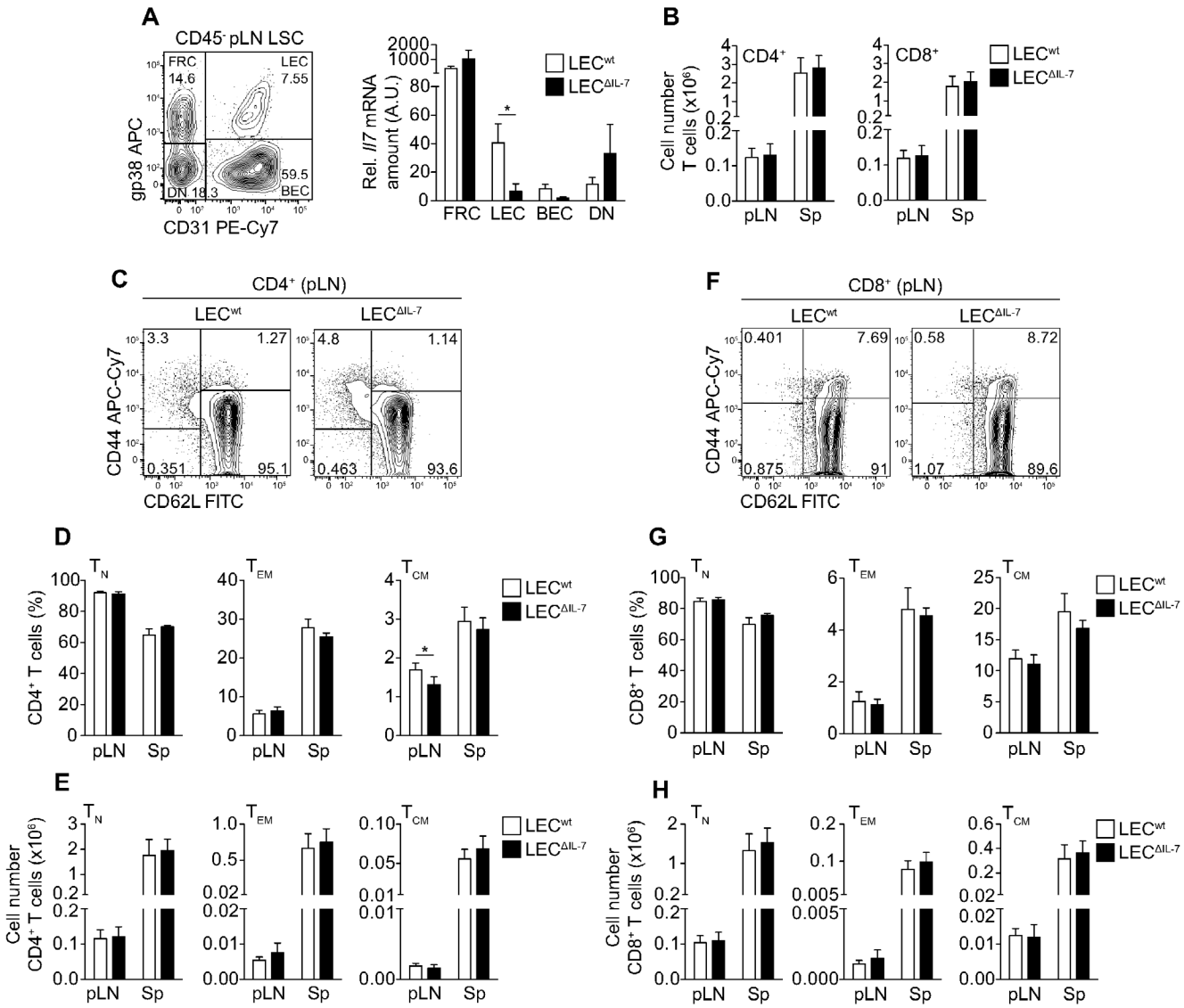

Figure 2. LEC-derived IL-7 is dispensable for peripheral T cell homeostasis. (A) Based on their differential expression of gp38 and CD31, live TER-119$^-$CD45$^-$ pLN LSCs can be subdivided into gp38$^+$CD31$^-$ FRCs, gp38$^+$CD31$^+$ LECs, gp38$^-$CD31$^+$ BECs, and gp38$^-$CD31$^-$ DNs. Shown is a representative contour plot from LEC$^{\Delta IL\text{-}7}$ mice; numbers indicate percentages. The indicated LSC subsets were purified by flow cytometry from LNs of LEC^{wt} (Lyve1-Cre$^+$IL-7$^{-/wt}$ and Lyve1-Cre$^-$IL-7$^{wt/wt}$) and LEC$^{\Delta IL\text{-}7}$ (Lyve1-Cre$^+$IL-7$^{-/fl}$) mice. Three independent sorts with pooled pLNs from three to four mice per group (in total nine to ten mice per group) were performed. Once, cells from two sorts were pooled. Relative *Il7* mRNA amounts were determined by RT-qPCR in relation to *Hprt*. Data displayed in the bar diagram are representative of two data points per group analyzed in two independent RT-qPCR experiments and show mean ± SEM of triplicates. Statistical significances were tested using a nonparametric two-tailed Mann–Whitney *U*-test (*$p \leq 0.05$). (B) Absolute numbers of CD3$^+$CD4$^+$ and CD3$^+$CD8$^+$ T cells were determined in pLNs and spleen (Sp). (C, D, F, and G) Frequencies and (E and H) absolute numbers of naive (T_N; CD44^{lo}CD62L^{hi}), effector memory (T_{EM}; CD44^{hi}CD62L^{lo}) and central memory (T_{CM}; CD44^{hi}CD62L^{hi}) T cells were determined after gating on (C–E) CD3$^+$CD4$^+$ and (F–H) CD3$^+$CD8$^+$ cells isolated from pLNs or spleen. (C and F) Shown are representative contour plots and numbers indicate percentages. (B–H) Data was collected using flow cytometry. (B–H) The data shown in bar diagrams represent mean ± SEM combined from 11–12 LEC^{wt} (Lyve1-Cre$^+$IL-7$^{-/wt}$) and LEC$^{\Delta IL\text{-}7}$ (Lyve1-Cre$^+$IL-7$^{-/fl}$) mice per group analyzed in six independent experiments. Statistical significances were tested using a non-parametric two-tailed Mann–Whitney *U*-test (*$p \leq 0.05$).

were detected in either case (Fig. 3E and G). Furthermore, TCR Vβ repertoires of CD4$^+$ and CD8$^+$ T cells were indistinguishable between FRC$^{\Delta IL\text{-}7}$ and FRC^{wt} mice (Fig. 3F and H). Hence, the size and diversity of the peripheral T cell pool is independent of pLN FRC-derived IL-7.

Next, we assessed whether LEC-derived IL-7 compensates for the lack of FRC-derived IL-7. For this purpose, FRC$^{\Delta IL\text{-}7}$ mice were crossed to LEC$^{\Delta IL\text{-}7}$ mice to generate double Cre-transgenic FRC/LEC$^{\Delta IL\text{-}7}$ mice lacking *Il7* gene expression in both, FRCs and LECs. Similar to LEC$^{\Delta IL\text{-}7}$ (Fig. 2B) or FRC$^{\Delta IL\text{-}7}$ mice (Fig. 3E and G), CD4$^+$ and CD8$^+$ T cells were equally abundant in FRC/LEC$^{\Delta IL\text{-}7}$ and FRC/LEC^{wt} controls (Fig. 3I and J) arguing against a compensatory effect of LEC-derived IL-7 in FRC$^{\Delta IL\text{-}7}$ mice.

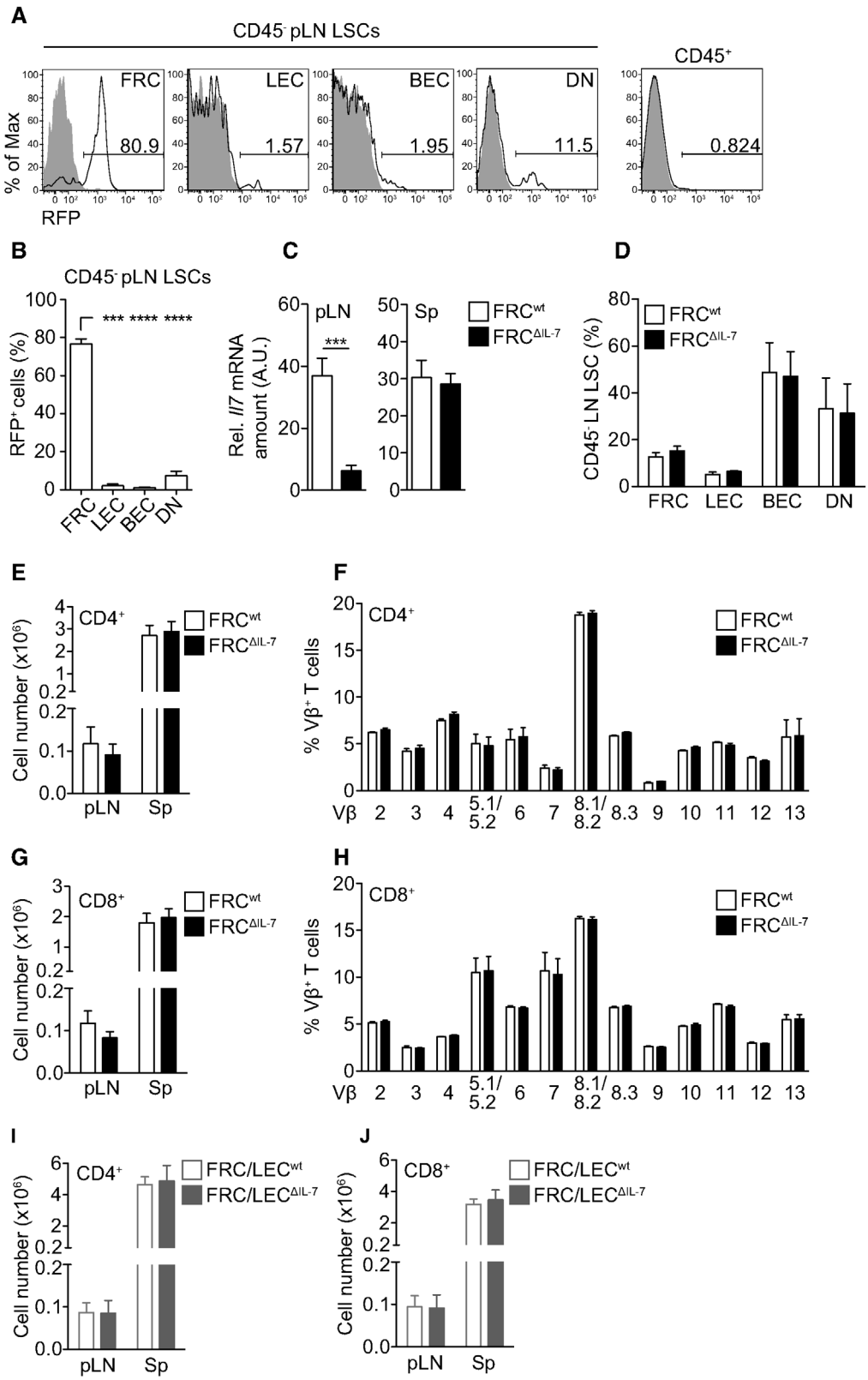

Figure 3. FRC-derived IL-7 does not affect size and diversity of the peripheral T cell pool. (A and B) Peripheral LNs were isolated from Prx1-Cre^{+}ROSA26^{RFP} (white curves) and Prx1-Cre^{-}ROSA26^{RFP} (grey curves) mice to determine recombination efficiency in live TER-119^{-}CD45^{-} LSCs and TER-119^{-}CD45^{+} leukocytes. (A) Numbers indicate percentages of RFP^{+} cells in Prx1-Cre^{+}ROSA26^{RFP} mice. (B) Data show percentages of RFP^{+} cells for the indicated LSC subsets (mean ± SEM). Data were pooled from four to five independent experiments with one to three mice per group. For FRCs, LECs, BECs, and DNs 13, 8, 13, and 13 individual data points were acquired, respectively. (C) Relative *Il7* mRNA amounts were determined

FRC-derived IL-7 determines T_{CM} abundance

Bcl-2 is a direct target of IL-7 [1] and is expressed at particularly high levels by $CD8^+$ T_M [36]. In order to test whether Bcl-2 expression is altered in the absence of FRC-derived IL-7, $CD8^+$ T_N and T_M derived from pLNs and spleens were analyzed. As shown in Fig. 4A, frequencies and numbers of $CD44^{hi}Bcl\text{-}2^{hi}$ $CD8^+$ T_M were significantly reduced in pLNs, but not spleens, of $FRC^{\Delta IL\text{-}7}$ mice. IL-7 conditions $CD8^+$ T cells for the IL-15-induced upregulation of Eomesodermin (Eomes) [37], a transcription factor promoting $CD8^+$ T_M differentiation [38]. As shown in Fig. 4B, $CD44^{hi}Eomes^{hi}$ $CD8^+$ T_M were strongly reduced in pLNs of $FRC^{\Delta IL\text{-}7}$ mice. Again, these differences between FRC^{wt} and $FRC^{\Delta IL\text{-}7}$ mice were most evident in pLNs. However, there was a tendency of reduced $CD8^+$ T_M frequencies and cell numbers in spleens of $FRC^{\Delta IL\text{-}7}$ mice (Fig. 4A and B).

To analyze this IL-7-dependent T_M defect in more detail, CD44 and CD62L expression was analyzed on $CD8^+$ T cells from pLNs and spleens of FRC^{wt} and $FRC^{\Delta IL\text{-}7}$ mice. Frequencies and numbers of $CD8^+$ $CD44^{lo}CD62L^{hi}$ T_N and $CD44^{hi}CD62L^{lo}$ T_{EM} were indistinguishable in pLNs and spleens of FRC^{wt} and $FRC^{\Delta IL\text{-}7}$ mice (Fig. 4C–E). In apparent contrast, frequencies of $CD8^+$ $CD44^{hi}CD62L^{hi}$ T_{CM} were significantly reduced in pLNs and spleens of $FRC^{\Delta IL\text{-}7}$ mice (Fig. 4D). With regard to absolute $CD8^+$ T_{CM} numbers, this difference between both mouse strains was limited to pLNs (Fig. 4E). $CD4^+$ T_N and $CD4^+$ T_{EM} frequencies and numbers were unaltered in pLNs and spleens of FRC^{wt} and $FRC^{\Delta IL\text{-}7}$ mice (Fig. 4F–H). Similar to $CD8^+$ T_{CM} (Fig. 4D), frequencies of $CD4^+$ T_{CM} were reduced in $FRC^{\Delta IL\text{-}7}$ pLNs but were only slightly affected in spleens (Fig. 4G). Absolute cell numbers were not significantly different in pLNs and spleens of both mouse strains (Fig. 4H). Hence, *Il7* gene inactivation in FRCs is associated with a reduction of $CD8^+$ T_{CM}, an effect that was by far less pronounced for $CD4^+$ T_{CM}.

The survival of both, T_N and T_{CM}, critically relies on IL-7 [1,4] suggesting that either incomplete *Il7* gene inactivation or the presence of non-pLN-derived IL-7 created IL-7 levels in $FRC^{\Delta IL\text{-}7}$ pLNs that were sufficient for T_N survival but too low for T_{CM} maintenance. However, this assumption would predict different efficacies of IL-7 utilization by T_N and T_{CM}. Consistent with this idea and recent data [39], IL-7 treatment induced a more efficient IL-7 receptor α (IL-7Rα; CD127) down-regulation by $CD8^+$ T_N compared to T_{CM} (Supporting Information Fig. 3A). IL-7R signaling leads to the phosphorylation of STAT5 that in turn regulates genes controlling T cell survival [40,41]. Interestingly, more pronounced IL-7Rα down-modulation by $CD8^+$ T_N (Supporting Information Fig. 3A) correlated with more efficient STAT5 phosphorylation (Supporting Information Fig. 3B). This argues for a more effective utilization of IL-7 by $CD8^+$ T_N and provides an explanation for their survival in $FRC^{\Delta IL\text{-}7}$ mice. Conversely, $CD8^+$ T_{CM} appear to require higher levels of FRC-derived IL-7 for survival.

Unimmunized adult mice contain virtual memory $CD8^+$ T cells ($CD8^+$ vT_M), which are generated independently of foreign antigen contact as a result of lymphopenia-induced proliferation (LIP) in the neonatal phase [42–47]. As we have shown previously, IL-7 promotes $CD8^+$ vT_M formation [45]. Whether and how FRC-derived IL-7 also affects the formation/maintenance of foreign antigen-specific $CD8^+$ T_{CM} was tested next. For this purpose, FRC^{wt} and $FRC^{\Delta IL\text{-}7}$ mice were reconstituted with TCR-transgenic $CD8^+$ OT-I T cells specific for the OVA-derived peptide SIINFEKL. In order to mimic a viral infection, recipient mice were immunized with a mixture of PolyI:C and SIINFEKL 24 h later. PolyI:C induces pro-inflammatory cytokines such as IFN-α/β and IFN-γ, which promote IL-7 upregulation [24,48] and the subsequent formation and maintenance of T_M [8,49]. Thirty days after vaccination the numbers of splenic $CD8^+$ OT-I T_M were comparable between FRC^{wt} and $FRC^{\Delta IL\text{-}7}$ mice (Fig. 4I). However, similar to the experiments shown above, T_{CM} frequencies were clearly reduced in $FRC^{\Delta IL\text{-}7}$ mice whereas T_{EM} appeared to be less dependent on FRC-derived IL-7 (Fig. 4J and K). This finding indicates that FRC-derived IL-7 helps to maintain both, virtual as well as foreign antigen-specific $CD8^+$ T_{CM}.

Discussion

In steady state, IL-7 is supposed to be produced at constant levels [50], mainly by radio-resistant stromal cells [1,51]. T_N and T_M express high levels of the IL-7R enabling them to remove IL-7 from the system continuously [50]. As soon as the peripheral T cell pool reaches a critical size, IL-7 production and consumption reach the equilibrium and the survival of additional T cells is prevented. Hence, the maintenance of T cell homeostasis relies on the competition for limiting amounts of IL-7 [14,50,52].

The seminal work by Link et al. identified LECs and FRCs as main sources of IL-7 in pLNs. Additionally, co-culture experiments

in pLNs (left) and spleens (Sp; right) of FRC^{wt} (Prx1-$Cre^+IL\text{-}7^{-/wt}$ and Prx1-$Cre^+IL\text{-}7^{wt/wt}$) and $FRC^{\Delta IL\text{-}7}$ (Prx1-$Cre^+IL\text{-}7^{-/fl}$ and Prx1-$Cre^+IL\text{-}7^{fl/fl}$) mice by RT-qPCR in relation to *Hprt*. Data are representative of five to nine mice per group analyzed in two to five independent RT-qPCR experiments and show mean ± SEM of triplicates. (D) Frequencies of viable TER-119^-CD45^- LSC subsets were determined in CD45-depleted LNs of FRC^{wt} (Prx1-$Cre^+IL\text{-}7^{-/wt}$) and $FRC^{\Delta IL\text{-}7}$ (Prx1-$Cre^+IL\text{-}7^{-/fl}$) mice. In three independent experiments, peripheral LNs of three mice were pooled and three individual data points were acquired for FRCs, LECs, BECs, and DNs. Shown are pooled results (mean ± SEM). (E and G) Absolute numbers and the (F and H) composition of the Vβ TCR repertoire were determined for (E and F) $CD3^+CD4^+$ and (G and H) $CD3^+CD8^+$ T cells in (E and G) pLN/Sp and (F and H) Sp of FRC^{wt} (Prx1-$Cre^+IL\text{-}7^{wt/wt}$) and $FRC^{\Delta IL\text{-}7}$ (Prx1-$Cre^+IL\text{-}7^{fl/fl}$) mice by flow cytometry. Data (mean ± SEM) were pooled from (E and G) three independent experiments with a total of 11 mice per group and (F and H) two independent experiments with a total of six mice per group. (I and J) Absolute numbers of (I) $CD3^+CD4^+$ and (J) $CD3^+CD8^+$ T cells were determined in pLNs and Sp of FRC/LEC^{wt} (Prx1-Cre^+Lyve1-$Cre^-IL\text{-}7^{-/wt}$) and FRC/$LEC^{\Delta IL\text{-}7}$ (Prx1-Cre^+Lyve1-$Cre^+IL\text{-}7^{-/fl}$) mice. Data (mean ± SEM) were pooled from four to six independent experiments with a total of 10–11 mice per group. (A, B, D–J) Data were analyzed using flow cytometry. (C–J) Statistical significances were tested using a non-parametric two-tailed Mann–Whitney *U*-test (***$p \leq 0.001$; ****$p \leq 0.0001$).

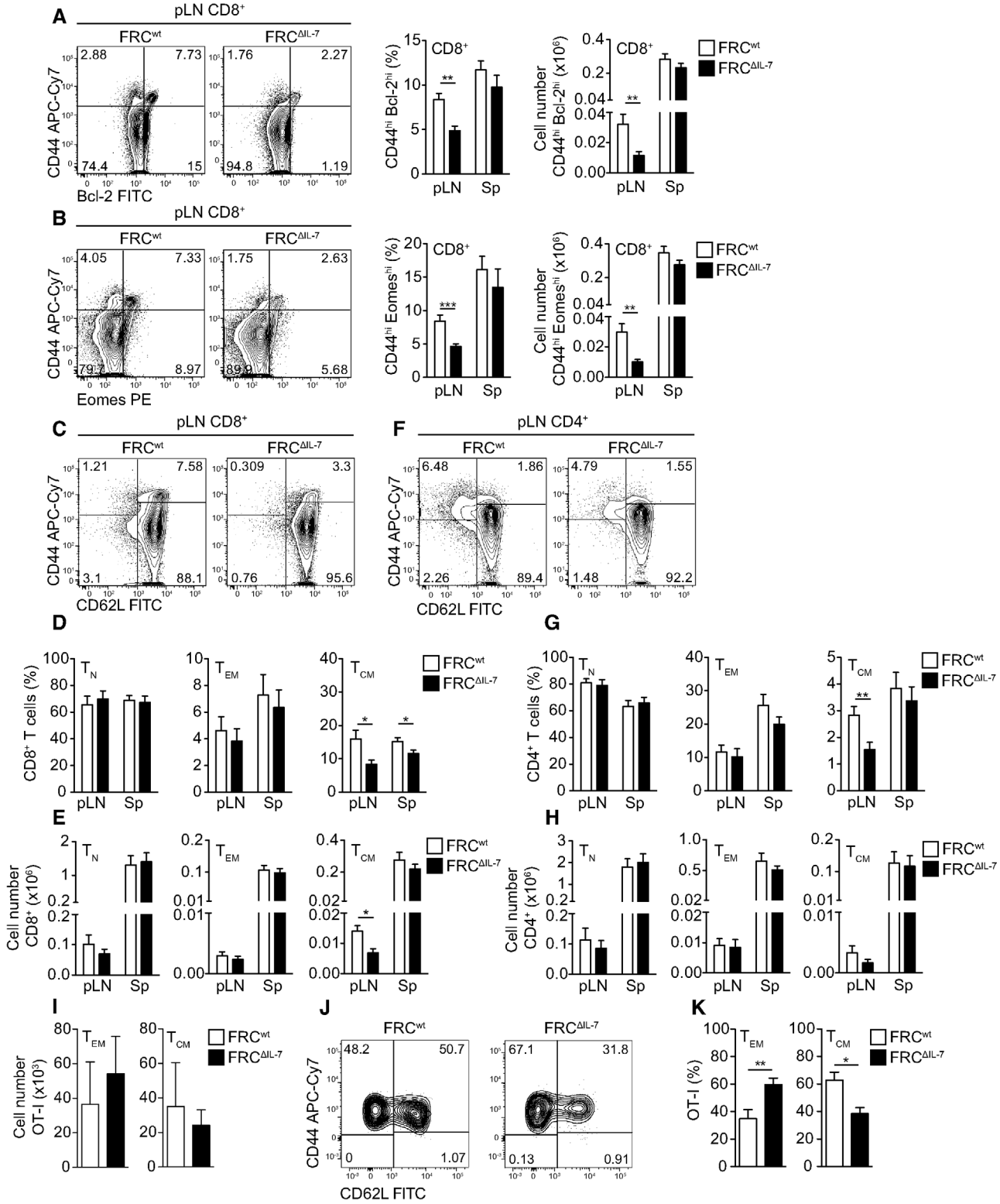

Figure 4. FRC-derived IL-7 determines T_{CM} abundance in pLNs. (A–E) $CD3^+CD8^+$ and (F–H) $CD3^+CD4^+$ T cells from pLNs and spleens (Sp) of FRC^{wt} ($Prx1\text{-}Cre^+IL\text{-}7^{wt/wt}$) and $FRC^{\Delta IL\text{-}7}$ ($Prx1\text{-}Cre^+IL\text{-}7^{fl/fl}$) mice were analyzed for their expression of the indicated molecules. (A, B, C, and F) Shown are representative contour plots and numbers indicate percentages. Bar diagrams represent percentages or numbers of (A) $CD44^{hi}Bcl\text{-}2^{hi}$, (B) $CD44^{hi}Eomes^{hi}$ cells or (D, E, G, H) T_N ($CD44^{lo}CD62L^{hi}$), T_{EM} ($CD44^{hi}CD62L^{lo}$), and T_{CM} ($CD44^{hi}CD62L^{hi}$). (A–H) Data in bar diagrams represent pooled results (mean ± SEM) from 10–11 mice combined and analyzed in three independent experiments. (I–K) $FRC^{\Delta IL\text{-}7}$ ($Prx1\text{-}Cre^+IL\text{-}7^{fl/fl}$) and FRC^{wt} ($Prx1\text{-}Cre^+IL\text{-}7^{wt/wt}$) mice (all $Thy1.2^+$) received 7×10^5 naive $CD8^+Thy1.1^+$ OT-I T cells. Twenty-four hours later, recipient mice were vaccinated

revealed that FRC-derived IL-7 promotes T_N survival [9] suggesting that circulating T_N receive IL-7-dependent survival signals in pLNs [14–17]. Besides its impact on T_N homeostasis, IL-7 also promotes the formation and maintenance of other pLN-homing immune cells including $CD8^+$ T_{CM} [1,8,40] and $ROR\gamma t^+$ type 3 innate lymphoid cells (ILC3) [53,54]. Therefore, a common pool of FRC-derived IL-7 is supposed to regulate homeostasis of multiple immune cells in pLNs [17].

There is accumulating evidence that $CD8^+$ T_N and T_M pools are regulated independently [55–57] indicating that they colonize different ecological niches [55–57]. In the immune system, ecological niches are defined by the combination of resources affecting the survival and function of a particular immune cell population [57]. In order to limit competition and enable the simultaneous survival of multiple immune cell types, ecological niches must be segregated. However, niche segregation of $CD8^+$ T_N and T_{CM} appears to be incomplete as suggested by their common IL-7 dependence [40,56]. Nevertheless, we do not know yet if niche segregation involves the IL-7-dependent spatial separation of both cell types. The uneven distribution of IL-7-producing FRCs [29,58] suggests that, similar to chemokines [59,60], areas of high and low IL-7 density exist in pLNs. Based on their differential IL-7 demands, this assumption would predict the accumulation of $CD8^+$ T_N and T_{CM} in separate pLN regions. Of note, the degree of local $CD8^+$ T_N and T_{CM} segregation in pLNs varies strongly between experimental systems [61,62]. Whether this context-dependent effect correlates with the presence or absence of IL-7-producing FRCs in particular regions is still unclear since, at least to our knowledge, reliable reagents for IL-7 protein detection in pLNs are still missing.

Although we cannot fully exclude that different anatomical locations modulate distinct aspects of IL-7-dependent $CD8^+$ T_N and T_{CM} homeostasis, our results indicate that variable IL-7 sensitivities of $CD8^+$ T_N and T_{CM} contribute to the segregation of their ecological niches. In agreement with a recent study [39], we confirmed that IL-7R signaling is less efficient in $CD8^+$ T_{CM}. In a situation of limited IL-7 availability, this property would provide an explanation for the reduction of virtual as well as foreign antigen-specific $CD8^+$ T_{CM} in $FRC^{\Delta IL\text{-}7}$ mice. Furthermore, our results are in line with the current paradigm of IL-7-dependent T cell homeostasis proposing that the optimized utilization of limiting IL-7 amounts is prerequisite for the survival of the greatest possible number of IL-7-dependent immune cells [63]. Based on this model, the degree of competition between different IL-7-consuming cells would be restricted and the limited space within pLNs would be used most optimally [14,50].

The insensitivity of T_N to FRC-specific *Il7* inactivation may be due to the fact that T_N are anyway capable of surviving short phases of IL-7 deficiency [63]. Indeed, IL-7 binding induces the down-modulation of IL-7R expression by T_N more rapidly than by T_{CM} rendering them insensitive to further IL-7 signals [63]. This effect is transient and appears to fulfill at least two functions. First, the amount of IL-7 consumed by a single T_N is restricted thereby optimizing IL-7 availability for other immune cells [63]. Second, permanent IL-7R signaling would cause chronic T cell activation and subsequent activation-induced cell death [64]. Keeping in mind that (i) multiple organs produce IL-7 [24,25] and (ii) T_N continuously circulate through the body, they may tolerate the partial IL-7-deficiency in $FRC^{\Delta IL\text{-}7}$ pLNs because they received critical IL-7 signals elsewhere. Alternatively, incomplete *Il7* gene inactivation in $FRC^{\Delta IL\text{-}7}$ pLNs may allow the production of residual IL-7, which is just sufficient to promote local T_N survival. In any case, our data demonstrate that T_{CM} and T_N do not tolerate the reduction of IL-7 in $FRC^{\Delta IL\text{-}7}$ pLNs equally well. As shown for polyclonal $CD8^+$ T cells in the steady state and for $CD8^+$ OT-I T cells after vaccination, T_{CM} prove to be particularly sensitive to IL-7 ablation in FRCs. However, $CD8^+$ T_{CM} are only partially reduced in $FRC^{\Delta IL\text{-}7}$ mice. Whether this is due to the survival of $CD8^+$ T_{CM} subsets with reduced IL-7 demands remains to be shown in the future.

When we compared $FRC^{\Delta IL\text{-}7}$ and FRC^{wt} pLNs, we did not observe any obvious differences (Supporting Information Fig. 2A–C). T and B lymphocyte distribution, stromal cell localization, and relative distances between FRCs and lymphocytes appeared normal in $FRC^{\Delta IL\text{-}7}$ mice (Supporting Information Fig. 2A–C). Furthermore, chemokine expression was comparable between $FRC^{\Delta IL\text{-}7}$ and FRC^{wt} pLNs (Supporting Information Fig. 2D) and ILC3 contributing to the IL-7-dependent regulation of T cell homeostasis [51,54,65] were similarly abundant (Supporting Information Fig. 2E). Hence, our findings argue for normal LN development and function in the absence of FRC-derived IL-7. This strongly suggests that the reduction of T_{CM} in $FRC^{\Delta IL\text{-}7}$ results from a lack of IL-7-dependent homing/survival signals rather than structural and/or functional alterations of $FRC^{\Delta IL\text{-}7}$ pLNs.

In summary, we provide evidence that IL-7 produced by pLN FRCs regulates T cell homeostasis. As opposed to the current model, our data demonstrate that pLN FRC-derived IL-7 is of limited importance for the local and systemic survival of T_N. On the contrary, the maintenance of T_{CM} critically relies on steady state levels of FRC-derived IL-7 suggesting that T_N and T_{CM} colonize different ecological niches in vivo.

Material and Methods

Mice

Prx1-Cre [66] (stock no. 005584) and Lyve1-Cre [30] (stock no. 012601) mice were purchased from The Jackson Laboratory.

i.v. with a mixture of 50 μg SIINFEKL and 50 μg PolyI:C. Thirty days post vaccination, recipient splenocytes were analyzed by flow cytometry. (I) Cell numbers and (K) frequencies of T_{EM} ($CD44^{hi}CD62L^{lo}$) and T_{CM} ($CD44^{hi}CD62L^{hi}$) were determined after gating on $CD8^+Thy1.1^+$ OT-I T cells. (J) Shown are representative contour plots and numbers indicate percentages. (I and K) Shown are pooled results (mean ± SEM) from eight to nine mice analyzed in three independent experiments. (A–K) Data were analyzed using flow cytometry. Statistical significances were tested using a non-parametric two-tailed Mann–Whitney *U*-test ($^*p \le 0.05$; $^{**}p \le 0.01$; $^{***}p \le 0.001$).

Together with IL-7$^{-/-}$ [3], PGK-Cre [27], Flpo [67], Rag1$^{-/-}$ Thy1.1^{+} OT-I [68], and ROSA26^{RFP} [33] mice, they were maintained under specific pathogen-free conditions at the central animal facility of the Medical Faculty of the Otto-von-Guericke-University Magdeburg. Whenever possible, control littermates were used. Experimental procedures were approved by the relevant animal experimentation committee and performed in compliance with international and local animal welfare legislations (Landesverwaltungsamt Sachsen-Anhalt Permit Number: 42502-2-1288 UniMD).

Generation of IL-7$^{fl/fl}$ mice and genotyping

The C57BL6/N (B6) embryonic stem cell (ES) line JM8A3.N1 harboring the "knockout-first" allele *Il7*$^{tm1a(EUCOMM)Wtsi}$ was provided by The European Conditional Mouse Mutagenesis Program (EUCOMM). Mice harboring the *Il7*$^{tm1a(EUCOMM)Wtsi}$ allele were generated by standard blastocyst injection and crossed to Flpo-transgenic mice [67] in order to remove the FRT-flanked part of the targeting construct (Supporting Information Fig. 1A). Resulting mice harboring floxed *Il7* alleles (*Il7*^{fl}) were crossed to the indicated Cre-transgenic mice in order to delete exons 3 and 4. Mice were genotyped by PCR using the forward primer 5'-AGAGGATGCAGGGACACATCTGCC-3 (upstream FRT site 1), the reverse primers 5'-ATTTTCCTGATTCTACTTACTGGC-3' (upstream exon 3) and 5'-CAACGGGTTCTTCTGTTAGTCC-3' (downstream FRT site 1) exhibiting a 445 bp band for the *Il7*$^{tm1a(EUCOMM)Wtsi}$ allele, a 680 bp band for the floxed *Il7* allele, and a 523 bp band for the WT allele.

Cell isolation

To obtain single cell suspensions from pLNs and spleens, organs were forced through metal strainers in PBS/2 mM EDTA (Carl Roth) and erythrocytes were lysed. For erythrocyte lysis, spleen cells were re-suspended in ammonium-chloride-potassium lysis buffer for 90 s followed by the addition of RPMI 1640 (Biochrom) containing 10% (v/v) FCS (PAN Biotech) and 1% (v/v) penicillin/streptomycin (P/S; Gibco). After centrifugation, spleen cells were re-suspended in PBS/2 mM EDTA and filtered through 40 μm cell strainers (Corning, Durham, NC).

For LSC and ILC isolation, fat-free pLNs were cut into small (1 × 1 mm) pieces in RPMI 1640/10% FCS/1% P/S. Peripheral LN fragments were vortexed and the supernatant was removed after the organ pieces had settled. This process was repeated three times. Cells in the supernatant were collected and ILCs were analyzed by flow cytometry. pLN fragments were transferred into 12-well plates containing 1 mL digestion medium I (0.2 mg/mL Collagenase P [Roche], 0.2 mg/mL Dispase II [Roche], 10 μg/mL DNase I [Sigma], and 5 μg/mL Latrunculin B [Calbiochem] in RPMI 1640 supplemented with 10% FCS/1% P/S). After incubation for 30 min at 37°C and 5% (v/v) CO_2, 1 mL digestion medium II (0.4 mg/mL Collagenase P, 0.2 mg/mL Dispase II, 10 μg/mL DNase I, and 5 μg/mL Latrunculin B in RPMI 1640/10% FCS/1 % P/S) was added and the samples were re-suspended. After incubation for 30 min at 37°C and 5% CO_2, 0.5 mL RPMI 1640/10% FCS/1% P/S/ 10 mM EDTA was added to stop digestion. Cell suspensions were filtered through 70 μm cell strainers and cells were washed with PBS/2 mM EDTA. Cells were resuspended in PBS/2 mM EDTA and filtered through 40 μm cell strainers.

Adoptive T cell transfer

Naive (CD44^{lo}CD62L^{hi}) CD8^{+} T cells (Supporting Information Fig. 6C) expressing a transgenic TCR (Vα2Vβ5) specific for the chicken OVA-derived, H2-K^{b}–restricted peptide OVA$_{257–264}$ (SIINFEKL), were isolated from LNs and spleen of Rag1$^{-/-}$ Thy1.1^{+} OT-I mice using CD8a-specific MicroBeads and AutoMACS (Miltenyi Biotec) according to the manufacturer's recommendations. Thy1.2^{+} recipients received 4–7 × 10^{5} OT-I T cells (purity > 81.7%) via i.v. injection into the tail vein. Twenty-four hours after T cell transfer recipient mice were immunized with a mixture of 50 μg SIINFEKL (Biosyntan) and 50 μg PolyI:C (Invivogen).

In vitro IL-7 stimulation

Single cell suspensions of peripheral and mesenteric lymph nodes were adjusted to 5 × 10^{6} cells/mL and incubated for 30 min at 37°C and 5% CO_2 in RPMI 1640 supplemented with 10% FCS/1% P/S/2 mM L-glutamine (Gibco)/1 mM sodium pyruvate (Gibco)/0.1 mM HEPES (Gibco)/50 μM 2-mercaptothanol (Sigma) and 1 ng/mL recombinant mouse (protein carrier free) IL-7 (EBioscience, Thermo Fisher Scientific).

Flow cytometry cell sorting of LSCs

LSCs were isolated from peripheral and mesenteric lymph nodes as described above. LN cells were incubated with purified anti-CD16/32 (2.4G2 ATCC® HB-197™) in staining buffer (PBS/0.5% [w/v] BSA (AppliChem)/2 mM EDTA) for 10 min at 4°C. Subsequently, cells were stained with biotinylated CD45- and TER-119-specific antibodies in staining buffer containing anti-CD16/32 for 30 min at 4°C. CD45^{+} and TER-119^{+} cells were depleted using Dynabeads Biotin Binder (Invitrogen). In brief, cells were re-suspended in staining buffer to 1 × 10^{7} cells/mL and 50 μL pre-washed magnetic beads were added. Cells were incubated for 30 min at 4°C under gentle rotation and CD45^{+} and TER-119^{+} cells were removed subsequently using a DynaMag-15 (Thermo Fisher Scientific). Remaining cells were stained with fluorochrome-labeled gp38- and CD31-specific antibodies as well as streptavidin-FITC for 30 min at 4°C. Finally, after washing with PBS/2 mM EDTA, the cells were re-suspended in RPMI 1640/10% FCS/1% P/S. For dead cell exclusion, 7-aminoactinomycin D (7-AAD; BioLegend) was added 5 min prior to cell sorting using a FACSARIA III (Becton Dickinson). Live (7-AAD^{-}),

TER-119$^-$CD45$^-$ LSC subsets were sorted based on their differential gp38/CD31 expression. Purities of the indicated LSC subsets were >73.3 % (data not shown).

Flow cytometry

The following reagents were purchased from BioLegend: anti-mouse Bcl-2 (10C4), CD3 (145-2C11), CD3 (17A2), CD4 (RM4-5), CD5 (53-7.3), CD8a (53-6.7), CD11c (N418), CD19 (6D5), CD44 (IM7), CD45 (30-F11), CD62L (MEL-14), CD127 (A7R34), gp38 (8.1.1), Gr1 (RB6-8C5), NK1.1. (PK136), TER-119 (TER-119), Thy1.1 (OX-7), Vα2 (B20.1), 7-AAD viability staining solution, and streptavidin-FITC. Anti-mouse CD31 (390), Eomes (Dan11mag), and RORγ(t) (B2D) were purchased from eBioscience. Anti-mouse CD45R (B220; RA3-6B2) and the anti-mouse TCR Vβ screening panel were purchased from BD Biosciences. Prior to staining with fluorochrome-labeled antibodies, single cell suspensions were incubated with 50 μL of anti-mouse CD16/32 in staining buffer for 10 min at 4°C. Afterward, cells were incubated with 50 μL of fluorochrome-labeled antibodies diluted in anti-CD16/32 containing staining buffer. After incubation for 30 min at 4°C, cells were washed with 200 μL PBS/ 2 mM EDTA. For intranuclear stainings (except pSTAT5), samples were processed using the FoxP3/Transcription Factor Staining Buffer Set (eBioscience, Thermo Fisher Scientific) according to the manufacturer's recommendations. For staining of pSTAT5, cell samples were fixed for 30 min at 4°C with Fixation Buffer (BioLegend) and washed with 200 μL Intracellular Staining Permeabilization Wash Buffer (BioLegend). Subsequently, cells were incubated with anti-mouse pSTAT5 Y694 (47; BD Biosciences) in wash buffer for 30 min at 4°C, washed with 200 μL Wash Buffer and finally resuspended in PBS/2 mM EDTA prior to analysis. For LSC analyses, 7-AAD was added 5 min prior to data acquisition. Samples were measured on a LSRFortessa (Becton Dickinson) and analyzed with FlowJo 9/10 software (FlowJo, LLC) according to the "Guidelines for the use of flow cytometry and cell sorting in immunological studies" [69]. Individual gating strategies are depicted in Supporting Information Figs. 1, 2, and 4–6.

Reverse transcriptase PCR (RT-PCR) and real-time quantitative PCR (RT-qPCR)

Colon samples were transferred into CK14 2 mL tubes (Peqlab/VWR) containing 700 μL TRIzol reagent (Invitrogen) and homogenized in a Precellys 24 homogenizer (Peqlab/VWR). Peripheral LNs were transferred into CK14 0.5 mL tubes (Peqlab/VWR) containing 200 μL TRIzol reagent and homogenized. Sorted LSCs were re-suspended in 500 μL TRIzol reagent. For RNA extraction, chloroform (Sigma–Aldrich) was added and total RNA was isolated according to the manufacturer's instructions.

Isolated RNA was quantified by photometric Nanodrop (Thermo Fisher Scientific) measurement. RNA was reverse-transcribed using random hexamer primers and the advantage RT-for-PCR kit (Takara Clontech) according to the manufacturer's instructions.

For RT-PCR analyses of colon samples, the Taqman® Gene Expression Master Mix (Thermo Fisher Scientific) and the following TaqMan® Gene Expression Assays (Thermo Fisher Scientific) were used according to the manufacturer's instructions: *Il7* (FAM-MGB probe Mm01295804_m1) and *Hprt* (FAM-MGB probe Mm00446968_m1). PCR products were analyzed by agarose gel electrophoresis.

For RT-qPCR analyses of sorted LSCs and whole pLNs, the Taqman® Gene Expression Master Mix (Thermo Fisher Scientific) and the following TaqMan® Gene Expression Assays (Thermo Fisher Scientific) were used according to the manufacturer's instructions: *Ccl19* (FAM-MGB probe Mm00839967_g1), *Ccl21* (FAM-MGB probe Mm03646971_gH), *Cxcl9* (FAM-MGB probe Mm000434946_m1), *Cxcl10* (FAM-MGB probe Mm00445235_m1), *Cxcl13* (FAM-MGB probe Mm00444534_m1), *Il7* (FAM-MGB probe Mm01295805_m1), and *Hprt* (FAM-MGB probe Mm00446968_m1). Samples were analyzed in triplicates and C_T values were exported from the ABI PRISM 7000 (Applied Biosystems) sequence detection system. The relative quantifications were calculated according to the ΔC_T method.

Automated multidimensional fluorescence microscopy by multi-epitope-ligand cartography

Multi-epitope-ligand cartography (MELC) was performed as described previously [70]. Briefly, pLNs were embedded into Tissue-Tek® O.C.T.™ compound (Sakura Finetek), frozen on dry ice, and stored at –80°C. Ten micrometer cryo-sections adhered to silane-coated cover slides (Thermo Fisher Scientific) were fixed with PBS/2% (w/v) paraformaldehyde (Sigma–Aldrich), permeabilized with PBS/0.2% (v/v) Triton-X-100 (Carl Roth) and blocked with PBS/1 % (w/v) BSA (Sigma–Aldrich) + 30% (v/v) normal goat serum (Invitrogen). Tissue samples were transferred to an inverted wide-field fluorescence microscope (Leica DMi8, 20× air lens NA 0.80; Leica Microsystems). The automated cyclic robotic process started with the incubation of the first fluorochrome-labeled antibody (tag). After a series of washing steps, the fluorescence signals and a corresponding phase contrast image were acquired by a cooled charge-coupled device camera (Apogee KX4; Apogee Instruments). The specific signal of the given tag was removed by bleaching the fluorescent dye followed by recording of post-bleaching fluorescence signals and repetition of incubation-imaging-bleaching-cycle. The appropriate working dilutions, incubation times, and positions within the MELC experiment of the used tags (anti-mouse CD3 (17A2), CD31 (390), CD8a (53-6.7), gp38 (8.1.1), CD45 (30-F11), CD54 (YN1/1.7.4), CD44 (IM7), and CD45R/B220 (RA3-6B2) were purchased from BioLegend, anti-mouse CD4 (RM4-5) from BD Biosciences, PI from Sigma–Aldrich) were validated systematically using conditions suitable to MELC [70]. The series of fluorescence images produced by each tag were aligned pixel-wise using the corresponding phase

contrast images. The automated algorithm reaches an alignment accuracy of 0.1 pixels. Illumination faults of the images were corrected using flat-field correction. Post-bleaching images were subtracted from the following fluorescence tag images. Section artifacts were excluded as invalid by a manual mask-setting process. We developed pipelines for the Cell Profiler software package [71] in order to detect (i) all cells within the tissue section using the staining of PI, CD45, CD44, and CD54, and (ii) to create masks for gp38 and CD31 positive signals. Using these masks of gp38 and CD31 the FRC region was defined as $gp38^+$ and $CD31^-$. For each cell, the mean fluorescent intensity and the smallest distance to the reference region FRC was calculated. The resulting matrix of intensities and distances were exported into an FCS file and uploaded to the online cytometry analysis platform "cytobank.org" for multiparametric analysis.

Statistical analyses

Statistical analyses and graphical representations were performed using Prism 5.0d/f (GraphPad Software Inc.). Statistical significances were determined using non-parametric two-tailed Mann–Whitney *U* tests; $^{*}p \leq 0.05$; $^{**}p \leq 0.01$; $^{***}p \leq 0.001$; $^{****}p \leq 0.0001$.

Acknowledgements: T.S. designed and supervised the study with the help of L.K. and K.D.; L.K., K.D., U.B., A.W., J.M., and L.P. performed experiments and analyzed data; H.J.F. provided essential reagents; A.J.M. and U.K. analyzed and discussed the data; T.S. analyzed the data and wrote the manuscript with the help of the other co-authors. We thank R. Naumann, J. Giese, E. Denks, C. Kozowsky, G. Höbbel, J. Nichelmann, and M. Berger for support and K. Anastassiadis for PGK-Cre- and Flpo-transgenic mice. This work was supported by the Deutsche Forschungsgemeinschaft (Sonderforschungsbereiche TR36 (project B7; to T.S.), SFB854 (project B15; to U.K. and T.S.), and DFG priority program 1937 (project SCHU 2326/2-1; to T.S.).

Conflict of interest: The authors declare no competing financial or commercial interests.

References

1 **Schluns, K. S., Kieper, W. C., Jameson, S. C. and Lefrançois, L.**, *Nat. Immunol.* 2000. **1**: 426–432

2 **Boyman, O., Purton, J. F., Surh, C. D. and Sprent, J.**, *Curr. Opin. Immunol.* 2007. **19**: 320–326

3 **von Freeden-Jeffry, U., Vieira, P., Lucian, L. A., McNeil, T., Burdach, S. E. and Murray, R.**, *J. Exp. Med.* 1995. **181**: 1519–1526

4 **Tan, J. T., Dudl, E., LeRoy, E., Murray, R., Sprent, J., Weinberg, K. I. and Surh, C. D.**, *Proc. Natl. Acad. Sci. U. S. A.* 2001. **98**: 8732–8737

5 **Opferman, J. T., Letai, A., Beard, C., Sorcinelli, M. D., Ong, C. C. and Korsmeyer, S. J.**, *Nature* 2003. **426**: 671–676

6 **Wofford, J. A., Wieman, H. L., Jacobs, S. R., Zhao, Y. and Rathmell, J. C.**, *Blood* 2008. **111**: 2101–2111

7 **Jacobs, S. R., Michalek, R. D. and Rathmell, J. C.**, *J. Immunol.* 2010. **184**: 3461–3469

8 **Cui, G., Staron, M. M., Gray, S. M., Ho, P.-C., Amezquita, R. A., Wu, J. and Kaech, S. M.**, *Cell* 2015. **161**: 750–761

9 **Link, A., Vogt, T. K., Favre, S., Britschgi, M. R., Acha-Orbea, H., Hinz, B., Cyster, J. G. et al.**, *Nat. Immunol.* 2007. **8**: 1255–1265

10 **Ariel, A., Hershkoviz, R., Cahalon, L., Williams, D. E., Akiyama, S. K., Yamada, K. M., Chen, C. et al.**, *Eur. J. Immunol.* 1997. **27**: 2562–2570

11 **Banwell, C. M., Partington, K. M., Jenkinson, E. J. and Anderson, G.**, *Eur. J. Immunol.* 2000. **30**: 2125–2129

12 **Dai, Z. and Lakkis, F. G.**, *J. Immunol.* 2001. **167**: 6711–6715

13 **Dummer, W., Ernst, B., LeRoy, E., Lee, D. and Surh, C.**, *J. Immunol.* 2001. **166**: 2460–2468

14 **Takada, K. and Jameson, S. C.**, *Nat. Rev. Immunol.* 2009. **9**: 823–832

15 **Huang, H.-Y. and Luther, S. A.**, *Semin. Immunol.* 2012. **24**: 175–189

16 **Chang, J. E. and Turley, S. J.**, *Trends. Immunol.* 2015. **36**: 30–39

17 **Alexandre, Y. O. and Mueller, S. N.**, *Immunol. Rev.* 2018. **283**: 77–85

18 **Weninger, W., Crowley, M. A., Manjunath, N. and von Andrian, U. H.**, *J. Exp. Med.* 2001. **194**: 953–966

19 **Miller, C. N., Hartigan-O'Connor, D. J., Sup Lee, M., Laidlaw, G., Cornelissen, I. P., Matloubian, M., Coughlin, S. R. et al.**, *Int. Immunol.* 2013.

20 **Heufler, C., Topar, G., Grasseger, A., Stanzl, U., Koch, F., Romani, N., Namen, A. E. et al.**, *J. Exp. Med.* 1993. **178**: 1109–1114

21 **Watanabe, M., Ueno, Y., Yajima, T., Iwao, Y., Tsuchiya, M., Ishikawa, H., Aiso, S. et al.**, *J. Clin. Invest.* 1995. **95**: 2945–2953

22 **Tokoyoda, K., Egawa, T., Sugiyama, T., Choi, B.-I. and Nagasawa, T.**, *Immunity* 2004. **20**: 707–718

23 **Alp, Ö.S., Durlanik, S., Schulz, D., McGrath, M., Grün, J. R., Bardua, M., Ikuta, K. et al.**, *Eur. J. Immunol.* 2015.

24 **Shalapour, S., Deiser, K., Sercan, O., Tuckermann, J., Minnich, K., Willimsky, G., Blankenstein, T. et al.**, *Eur. J. Immunol.* 2010. **40**: 2391–2400

25 **Shalapour, S., Deiser, K., Kühl, A. A., Glauben, R., Krug, S. M., Fischer, A., Sercan, O. et al.**, *PLoS One* 2012. **7**: e31939

26 **Masopust, D. and Schenkel, J. M.**, *Nat. Rev. Immunol.* 2013. **13**: 309–320

27 **Lallemand, Y., Luria, V., Haffner-Krausz, R. and Lonai, P.**, *Transgenic. Res.* 1998. **7**: 105–112

28 **Turley, S. J., Fletcher, A. L. and Elpek, K. G.**, *Nat Rev. Immunol.* 2010. **10**: 813–825

29 **Hara, T., Shitara, S., Imai, K., Miyachi, H., Kitano, S., Yao, H., Tani-ichi, S. et al.**, *J. Immunol.* 2012. **189**: 1577–1584

30 **Pham, T. H. M., Baluk, P., Xu, Y., Grigorova, I., Bankovich, A. J., Pappu, R., Coughlin, S. R. et al.**, *J. Exp.Med.* 2010. **207**: 17–27

31 **Greenbaum, A., Hsu, Y.-M. S., Day, R. B., Schuettpelz, L. G., Christopher, M. J., Borgerding, J. N., Nagasawa, T. et al.**, *Nature* 2013. **495**: 227–230

32 **Cordeiro Gomes, A., Hara, T., Lim, V. Y., Herndler-Brandstetter, D., Nevius, E., Sugiyama, T., Tani-Ichi, S. et al.**, *Immunity* 2016. **45**: 1219–1231

33 **Luche, H., Weber, O., Nageswara Rao, T., Blum, C. and Fehling, H. J.**, *Eur. J. Immunol.* 2007. **37**: 43–53

34 **Castagnaro, L., Lenti, E., Maruzzelli, S., Spinardi, L., Migliori, E., Farinello, D., Sitia, G. et al.**, *Immunity* 2013. **38**: 782–791

35 **Golub, R., Tan, J., Watanabe, T. and Brendolan, A.**, *Trends. Immunol.* 2018. **39**: 503–514

36 **Grayson, J. M., Zajac, A. J., Altman, J. D. and Ahmed, R.**, *J. Immunol.* 2000. **164**: 3950–3954

37 **Li, Q., Rao, R. R., Araki, K., Pollizzi, K., Odunsi, K., Powell, J. D. and Shrikant, P. A.**, *Immunity* 2011. **34**: 541–553

38 **Banerjee, A., Gordon, S. M., Intlekofer, A. M., Paley, M. A., Mooney, E. C., Lindsten, T., Wherry, E. J. et al.**, *J. Immunol.* 2010. **185**: 4988–4992

39 **Kim, H. K., Chung, H., Kwon, J., Castro, E., Johns, C., Hawk, N. V., Hwang, S. et al.**, *Front. Immunol.* 2019.**10**

40 **Surh, C. D. and Sprent, J.**, *Immunity* 2008. **29**: 848–862

41 **Rochman, Y., Spolski, R. and Leonard, W. J.**, *Nat. Rev. Immunol.* 2009. **9**: 480–490

42 **Ichii, H., Sakamoto, A., Hatano, M., Okada, S., Toyama, H., Taki, S., Arima, M. et al.**, *Nat. Immunol.* 2002. **3**: 558–563

43 **Le Campion, A., Bourgeois, C., Lambolez, F., Martin, B., Leaument, S., Dautigny, N., Tanchot, C. et al.**, *Proc. Natl. Acad. Sci. U. S. A.* 2002. **99**: 4538–4543

44 **Min, B., McHugh, R., Sempowski, G. D., Mackall, C., Foucras, G. and Paul, W. E.**, *Immunity* 2003. **18**: 131–140

45 **Schüler, T., Hämmerling, G. J. and Arnold, B.**, *J. Immunol.* 2004. **172**: 15–19

46 **Haluszczak, C., Akue, A. D., Hamilton, S. E., Johnson, L. D., Pujanauski, L., Teodorovic, L., Jameson, S. C. et al.**, *J. Exp. Med.* 2009. **206**: 435–448

47 **Smith, N. L., Patel, R. K., Reynaldi, A., Grenier, J. K., Wang, J., Watson, N. B., Nzingha, K. et al.**, *Cell* 2018. **174**: 117–130.e14

48 **Sawa, Y., Arima, Y., Ogura, H., Kitabayashi, C., Jiang, J.-J., Fukushima, T., Kamimura, D. et al.**, *Immunity* 2009. **30**: 447–457

49 **Kaech, S. M., Tan, J. T., Wherry, E. J., Konieczny, B. T., Surh, C. D. and Ahmed, R.**, *Nat. Immunol.* 2003. **4**: 1191–1198

50 **Mazzucchelli, R. and Durum, S. K.**, *Nat. Rev. Immunol.* 2007. **7**: 144–154

51 **Martin, C. E., Spasova, D. S., Frimpong-Boateng, K., Kim, H.-O., Lee, M., Kim, K. S. and Surh, C. D.**, *Immunity* 2017. **47**: 171–182.e4

52 **Jameson, S. C.**, *Nat. Rev. Immunol.* 2002. **2**: 547–556

53 **Satoh-Takayama, N., Lesjean-Pottier, S., Vieira, P., Sawa, S., Eberl, G., Vosshenrich, C. A. J. and Di Santo, J. P.**, *J. Exp. Med.* 2010. **207**: 273–280

54 **Yang, J., Cornelissen, F., Papazian, N., Reijmers, R. M., Llorian, M., Cupedo, T., Coles, M. et al.**, *J. Exp. Med.* 2018.

55 **Freitas, A. A. and Rocha, B.**, *Annu. Rev. Immunol.* 2000. **18**: 83–111

56 **Almeida, A. R., Amado, I. F., Reynolds, J., Berges, J., Lythe, G., Molina-París, C. and Freitas, A. A.**, *Front. Immunol.* 2012. **3**: 125

57 **Veiga-Fernandes, H. and Freitas, A. A.**, *Trends. Immunol.* 2017. **38**: 777–788

58 **Repass, J. F., Laurent, M. N., Carter, C., Reizis, B., Bedford, M. T., Cardenas, K., Narang, P. et al.**, *Genesis* 2009. **47**: 281–287

59 **Ulvmar, M. H., Werth, K., Braun, A., Kelay, P., Hub, E., Eller, K., Chan, L. et al.**, *Nat. Immunol.* 2014. **15**: 623–630

60 **Jafarnejad, M., Zawieja, D. C., Brook, B. S., Nibbs, R. J. B. and Moore, J. E.**, *J. Immunol.* 2017. **199**: 2291–2304

61 **Kastenmüller, W., Brandes, M., Wang, Z., Herz, J., Egen, J. G. and Germain, R. N.**, *Immunity* 2013. **38**: 502–513

62 **Sung, J. H., Zhang, H., Moseman, E. A., Alvarez, D., Iannacone, M., Henrickson, S. E., de la Torre, J. C. et al.**, *Cell* 2012. **150**: 1249–1263

63 **Park, J. H., Yu, Q., Erman, B., Appelbaum, J. S., Montoya-Durango, D., Grimes, H. L. and Singer, A.**, *Immunity* 2004. **21**: 289–302

64 **Kimura, M. Y., Pobezinsky, L. A., Guinter, T. I., Thomas, J., Adams, A., Park, J.-H., Tai, X. et al.**, *Nat. Immunol.* 2013. **14**: 143–151

65 **Bank, U., Deiser, K., Finke, D., Hämmerling, G. J., Arnold, B. and Schüler, T.**, *J. Immunol.* 2016.

66 **Logan, M., Martin, J. F., Nagy, A., Lobe, C., Olson, E. N. and Tabin, C. J.**, *Genesis* 2002. **33**: 77–80

67 **Kranz, A., Fu, J., Duerschke, K., Weidlich, S., Naumann, R., Stewart, A. F. and Anastassiadis, K.**, *Genesis* 2010. **48**: 512–520

68 **Stoycheva, D., Deiser, K., Stärck, L., Nishanth, G., Schlüter, D., Uckert, W. and Schüler, T.**, *J. Immunol.* 2015. **194**: 553–559

69 **Cossarizza, A., Chang, H. D., Radbruch, A., Acs, A., Adam, D., Adam-Klages, S., Agace, W. W. et al.**, *Eur. J. Immunol.* 2019. **49**: 1457–1973

70 **Schubert, W., Bonnekoh, B., Pommer, A. J., Philipsen, L., Böckelmann, R., Malykh, Y., Gollnick, H. et al.**, *Nat. Biotechnol.* 2006. **24**: 1270–1278

71 **Carpenter, A. E., Jones, T. R., Lamprecht, M. R., Clarke, C., Kang, I. H., Friman, O., Guertin, D. A. et al.**, *Genome. Biol.* 2006. **7**: R100

Abbreviations: **Bcl-2**: B-cell lymphoma 2 · **BEC**: blood endothelial cell · **DN**: gp38$^-$ CD31$^-$ double negative cell · **Eomes**: eomesodermin · **FRC**: fibroblastic reticular cell · **ILC**: innate lymphoid cell · **LEC**: lymphatic endothelial cell · **LIP**: lymphopenia-induced proliferation · **LSC**: lymphoid stromal cell · **Pln**: peripheral LN · **T_{CM}**: central memory T cell · **T_M**: memory T cells · **T_N**: naive T cell · **vT_M**: virtual memory T cell

Full correspondence: Dr. Thomas Schüler, Institute of Molecular and Clinical Immunology, Medical Faculty, Otto-von-Guericke University, Leipziger Strasse 44, 39120 Magdeburg, Germany
e-mail: thomas.schueler@med.ovgu.de

The peer review history for this article is available at https://publons.com/publon/10.1002/eji.201948368

Received: 23/8/2019
Revised: 23/1/2020
Accepted: 7/2/2020
Accepted article online: 11/2/2020